Phys. Status Solidi B **251**, No. 9, 1945–1954 (2014) / **DOI** 10.1002/pssb.201350253

Part of Special Issue on
Semiconductor Spintronics

physica status solidi b
www.pss-b.com
basic solid state physics

Feature Article

Spin entanglement generation and detection in semiconductor nanostructures

Wolfgang Belzig[*,1] **and Adam Bednorz**[2]

[1] Department of Physics, University of Konstanz, 78457 Konstanz, Germany
[2] Faculty of Physics, University of Warsaw, ul. Hoża 69, 00-681 Warsaw, Poland

Received 7 October 2013, revised 20 December 2013, accepted 23 December 2013
Published online 14 February 2014

Keywords Bell inequality, cross correlations, entanglement, quantum manipulation, quantum noise

* Corresponding author: e-mail Wolfgang.Belzig@uni-konstanz.de, Phone: +49-7531-884782, Fax: +49-7531-883091

Entanglement, viz. the non-separability of quantum states, is a fundamental prediction of quantum mechanics, which is at odds with the classical perception of reality. Furthermore, it constitutes a resource for quantum computation and quantum communication. Electronic degrees of freedom in nanostructures – in particular the spin – constitute promising candidates to implement quantum information architectures in scalable solid state circuits. In this topical review, we will summarize some efforts to create and detect entanglement in such structures. We concentrate first on entanglement in double quantum dots, since they promise to be viable candidates to produce entanglement by confining electrons to a small interaction region. The quantitative detection of the entanglement through transport measurements can be done via current and noise. Secondly, we concentrate on the creation of spin entanglement at quantum point contacts, which has the advantage that the two electrons are automatically spatially separated. We discuss the possibility of performing a Bell test of non-local correlations. However, as we will point out, a reliable entanglement detection can be performed by current-correlation measurements, although they require some trust in the experimental setup. Finally, we present a hierarchy of mesoscopic Bell tests, which could be useful to evaluate theoretical proposals and experimental setups.

1 Introduction The recent years have seen a tremendous progress in the quantum manipulation of spin degrees of freedom in semiconductor nanostructures [1–3]. One motivation stems from the fact that it is believed that manipulating the spin degree of freedom of the electrons is less prone to heating effects, limiting standard electrostatic carrier density control based electronics. However, a huge problem in spin manipulation is the usual weak coupling of the spin to external fields, which can be controlled on nanoscale dimensions. Still, the manipulation of spin in nanoelectronic circuits offers another possibility of quantum coherent manipulation, which might have no classical analog. On one hand, the spin of an electron itself constitutes a quantum degree of freedom, which cannot be realized classically. However, a single spin also acts effectively as a simple magnetic moment of size $\mu_B\hbar/2$ and the behavior of the magnetic moment in external fields follows classical equations of motion like the Bloch equation. The quantum nature only comes into play if the spin is detected in a standard quantum mechanical projective measurement. This is, for example, the case if an electronic current is detected in a spin-polarized contact. However, the quantum information about the spin state bearing a certain direction on the Bloch sphere is lost since only the projection onto one predefined component/direction is measured.

The situation becomes entirely different if the many-particle aspects of electrons are taken into account. The many-particle wave function $\phi(1,2)$ introduces the concept of indistinguishable particles and hence the question of exchange of the arguments of the wave function. In particular, the wave function can be in a superposition of product states, which constitutes a so-called non-separable state. If the particles are sufficiently spatially separated, one speaks of entanglement. Such a state induces non-local correlations, which cannot be explained classically and has been a subject of research ever since the early days of quantum mechanics [4]. Considered to be a purely academic and unobservable

curiosity, this changed dramatically when Bell [5] showed that such correlations can be turned into a measurable test by violating a classical inequality for moments and thereby ruling out all classical explanations for the correlations. Since then numerous experiments have shown a violation of the Bell inequality [6]; however so far they have always been relying on one or another assumption [7–9]. Even more interest in entanglement arises from the fact that it constitutes a resource for quantum computing [10]. Since several setups for solid state architectures for quantum computing have been proposed, entanglement has also moved into the focus of current research.

In particular, using spins in quantum dots as quantum bits has attracted a tremendous interest after they had been proposed in Ref. [11]. Therefore, ways to produce and transport entangled electrons in semiconductors have been investigated. At an early stage double quantum dots were proposed to create entanglement with normal [12] or superconducting leads [13]. However, the question of the detection of a successful production of entanglement was at first left open. Later this turned into the focus of experimental and experimental activities. It will be one of our main concerns in this review of how to access observable consequences and, in particular, the question of which additional assumptions are necessary to show that indeed non-local quantum entanglement has been produced.

This review is composed of three parts. In the first part, we address the principle of entanglement and measures of entanglement in an abstract framework. Such abstract measures are useful in general discussions of entanglement, but in many cases are not directly related to measurable quantities. Nevertheless, one can indirectly probe these entanglement measures in transport experiments. In the second part, we will review the physics of two electrons in a double quantum dot, in particular their entanglement properties. Such entanglement can be quantified, but a measurement requires some indirect way to access the entanglement, e.g., by transport measurements. In the following, we review a method of extracting the concurrence in terms of an important interaction parameter by means of shot-noise measurements at the edge of the Coulomb blockade region. In the third part, we discuss entanglement creation by scattering of fermions at a quantum point contact, which has much formal equivalence to Andreev scattering at superconducting interfaces. The most common approach is to view this as some sort of electronic equivalent to photonic beam splitters and consider similar questions like the violation of Bell inequalities. We review the standard approach, which addresses this in terms of current-correlation functions, but will have to emphasize that second-order correlators are not sufficient to prove entanglement unless a given representation of the observables and states is assumed. We discuss the prospects of using higher-order correlation functions to achieve a loophole-free mesoscopic Bell test.

2 Entanglement and measures of entanglement

The notion of entanglement was introduced in the early days of quantum mechanics. It refers to the fact that a composite quantum system can be brought into a superposition of different product states. Hence, the state cannot be written as a product state of the two separate quantum systems. This introduced a correlation between two quantum systems, which can in principle be arbitrarily far apart. This has in fact triggered the question of whether such correlations, which constitute some kind of instantaneous interaction, are compatible with the requirements of special relativity.

The most generic entangled state is the so-called Einstein–Podolski–Rosen pair of two spin-1/2 particles:

$$|\mathrm{EPR}\rangle = \frac{1}{\sqrt{2}}\left(|\uparrow\downarrow\rangle - |\downarrow\uparrow\rangle\right). \tag{1}$$

Obviously, it is not possible to decompose this state into a product state. In many cases however it is more appropriate to describe a system in mixed state by a density matrix $\hat{\rho} = \sum_n p_n |n\rangle\langle n|$. Entanglement is now defined such that the density matrix cannot be decomposed into a sum of non-entangled pure states. This definition makes it difficult to determine if a given density matrix contains entanglement. A famous example is the so-called Werner state [14], given by

$$\hat{W} = \frac{1}{4}(1-\xi)\hat{1} + \xi\,|\mathrm{EPR}\rangle\,\langle\mathrm{EPR}|\,, \tag{2}$$

with $-1/3 \le \xi \le 1$. This state is entangled for $\xi > 1/3$, which follows from a finite concurrence and violates the Bell inequality for $\xi > 1/\sqrt{2}$ (both criteria will be defined later).

In many cases it is of interest to quantify the entanglement, e.g., to check the performance of a certain device or protocol to create entangled pairs or how long a certain entangled state survives if it is subject to decoherence. Several measures of entanglement exist in the literature and we list below only those which will be considered in semiconductor nanostructures.

2.1 Concurrence The concurrence [15] for a mixed state is defined via the eigenvalues $\{\lambda_i\}$ of the matrix $\hat{\rho}(\hat{\sigma}_y \otimes \hat{\sigma}_y)\hat{\rho}^*(\hat{\sigma}_y \otimes \hat{\sigma}_y)$ as

$$\mathcal{C} = \max\{0, \sqrt{\lambda_1} - \sqrt{\lambda_2} - \sqrt{\lambda_3} - \sqrt{\lambda_4}\}\,, \tag{3}$$

with $\lambda_1 \ge \lambda_{2,3,4}$. For pure states $\rho = |\psi\rangle\langle\psi|$ it is reduced to $\mathcal{C} = |\langle\psi|(\hat{\sigma}_y \otimes \hat{\sigma}_y)|\psi\rangle|$. The concurrence is zero for separable states and reaches the maximum of 1 for pure entangled states a'la $|\mathrm{EPR}\rangle$. Interestingly, for the Werner state defined above one finds the analytic result $\mathcal{C} = \max\{0, (3\xi - 1)/2\}$, which shows that the state is entangled for $\xi > 1/3$.

2.2 Entanglement of formation Loosely related to the concurrence is the so-called entanglement of formation [16], defined via

$$\mathcal{E}(\hat{\rho}) = -\sum_{\sigma=\pm} \frac{1}{2}(1\sigma\sqrt{1-\mathcal{C}^2}) \log_2 \left[\frac{1}{2}(1\sigma\sqrt{1-\mathcal{C}^2})\right]. \tag{4}$$

This entanglement measure has a physical meaning in that it can be seen as the fraction of pure singlet states in a given experiment which is necessary to produce the corresponding density matrix.

We consider the previously defined entanglement measured as quantum information theoretical constructions. They are useful for the quantification of entanglement and the general research on entangled states. However, a general difficulty lies in the fact that they are not easily related to measurable quantities or correlation functions of spin variables; one must at least assume a representation of the observables and the density matrix in a given Hilbert space.

2.3 General Bell test Entanglement is often mentioned as a non-local – and hence non-classical – feature of quantum states. However, the entanglement is usually defined using a particular quantum representation of a state and observables in a Hilbert space. If we cannot take the representation for granted then entanglement is not conclusive evidence of non-locality. Note that the representation itself is not measurable and so there may be a different representation in which the state is not entangled. Hence, tests of the non-local nature of a quantum correlation must be representation-free and based solely on the measurement statistics. The most known procedure is the Bell test, later improved by Clauser et al. [5, 6]. The test requires two separate parties, usually called Alice and Bob, each of them free to measure one of two possible quantities, $A_{1,2}$ and $B_{1,2}$, respectively. The results of the measurement must be dichotomic, ± 1 (if there are more results, we simply split them into two complementary sets and assign $+1$ to all results in one set and -1 in the complementary one). Then the following statistical inequality holds [5, 6]:

$$|\langle A_1B_1 + A_2B_1 + A_1B_2 - A_2B_2\rangle| \leq 2\,. \tag{5}$$

It is important that all correlations are measured with respect to the same probability distribution. On the other hand, this inequality is violated in quantum mechanics for the state (1) taking $\hat{A}_1 = \hat{\sigma}_A^0$, $\hat{A}_2 = \hat{\sigma}_A^{\pi/2}$, $\hat{B}_1 = \hat{\sigma}_B^{5\pi/4}$, $\hat{B}_2 = \hat{\sigma}_B^{3\pi/4}$, with $\hat{\sigma}^\phi = e^{i\phi}\,|{\downarrow}\rangle\langle{\uparrow}| + \text{h.c.}$ in the respective Hilbert space. Then $\langle\hat{\sigma}_A^\alpha\hat{\sigma}_B^\beta\rangle = -\cos(\alpha-\beta)$, so $\langle A_1B_1\rangle = \langle A_1B_2\rangle = \langle A_2B_1\rangle = -\langle A_2B_2\rangle = 1/\sqrt{2}$ and the left-hand side of (5) is equal to $2\sqrt{2} \geq 2$. Violation of the Bell inequality is also a proof of entanglement, but not all entangled states violate the Bell inequality, e.g., the state (2) is entangled without violation of (5) for $\xi \in [1/3, 1/\sqrt{2}]$. When claiming entanglement, one must trust the quantum representation of the observable operator $\hat{A} \to A$ and the quantum probability rule $\langle ABC\cdots\rangle = \langle\hat{A}\hat{B}\hat{C}\cdots\rangle = \mathrm{Tr}\hat{\rho}\hat{A}\hat{B}\hat{C}\cdots$ for commuting $\hat{A}$, $\hat{B}$, $\hat{C}$, and the state $\hat{\rho}$.

The violation of (5) has been confirmed experimentally [17, 18] albeit there are still loopholes in the interpretation of these experiments. For example, Alice and Bob may communicate during the measurement due to the small distance between them, which is commonly called the communication loophole (the underlying probability distribution may depend on the choice of observables). On the other hand, inefficient detectors, which see only a small fraction of the photons or other particles, lead to the detection loophole (equivalently, one can say the dichotomy assumption is not fulfilled because of the additional null event). Moreover, practical realizations of the state (1) may not be ideal enough to survive the detrimental effects of decoherence within the required time scale of measurements to violate the Bell inequality (5) without loopholes.

2.4 Assessment of entanglement The problem of quantifying entanglement has several aspects. There is the theoretical question of quantitative measure, which interestingly has so far been only answered conclusively for two qubits, while it is still being debated for entanglement of parties with three or more states. One common problem is, however, that the measures for bipartite entanglement above rely on nonlinear expectation values of the density matrix and therefore are not directly related to physical observables. Of course, the elements of the density matrix of a given system are in principle measurable. However, such a measurement requires an *a priori* assumption about the structure of the Hilbert space. In many cases, the system is deliberately designed to possess only the few number of states required to apply entanglement measures as above. This is, for example, the case of quantum dots, where the number of electrons can be determined by manipulation of the various gate electrodes. Although in the Coulomb blockade regime the number of electrons is fixed, to determine the structure of the available states in general needs further and independent verification.

3 Entanglement in double quantum dots One obvious appearance of entanglement in a mesoscopic structure is that of two electrons in a double quantum dot. It has first been theoretically proposed in Ref. [12]. The electron states are defined with respect to the orbitals of the two quantum dots. Originally they were assumed to be the orbitals of two harmonic potentials suitable for quantum dots defined by top gates in two-dimensional electron gases created in semiconductor heterostructures. However, in view of more recent realization of double quantum dots in carbon nanotubes or semiconductor nanowires [19–21], different degrees of freedom, like the spin, moved into the focus of research.

3.1 Two-electron entanglement In a double dot as illustrated in Fig. 1 the single-electron states are characterized as symmetric and antisymmetric orbitals $\phi_\pm = (\phi_\mathrm{L} \pm \phi_\mathrm{R})/\sqrt{2}$ with corresponding creation operators $d^\dagger_{\pm\sigma}$ for an electron with spin σ. This allows us to define the two-electron states

$$|\mathrm{S}\rangle = \frac{1}{\sqrt{1+\phi^2}}(d^\dagger_{+\uparrow}d^\dagger_{+\downarrow} - \phi d^\dagger_{-\uparrow}d^\dagger_{-\downarrow})|0\rangle\,. \tag{6}$$

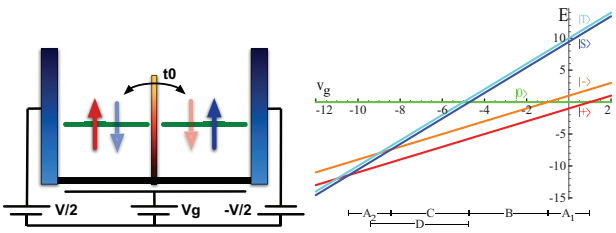

Figure 1 Energy of the states as a function of gate voltage V_g in units of t_0. The capital letters correspond to the regions in Fig. 2. The parameters are chosen as in Fig. 2.

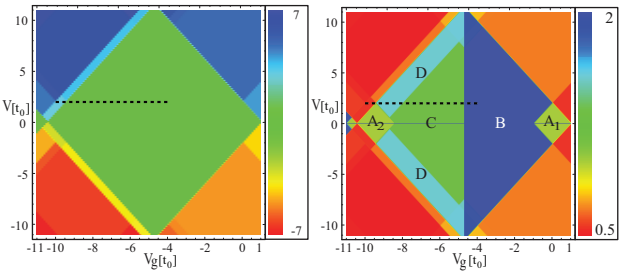

Figure 2 Current (left) and Fano factor (right) in the one-electron blockade regime as a function of gate voltage V_g and bias voltage V. The current is given in units of $e\gamma$, where γ is the base tunneling rate. Note the various plateaus in the Fano factor within the blockade regime, which are invisible in the current. The letters label the subregions as referred to in the main text. In this plot we use the parameters $u_H = 17t_0$, $u_{12} = 10t_0$, $\gamma_L = \gamma_R = \gamma$, and $k_B T = 0.01t_0$ (and hence $J = 0.24t_0$ and $\phi = 0.79$).

Expressed in terms of the dot orbitals, the state takes the form

$$|\mathrm{S}\rangle = \frac{1}{\sqrt{1+\phi^2}}\left[(1+\phi)(d^\dagger_{\mathrm{L}\uparrow}d^\dagger_{\mathrm{R}\downarrow} - d^\dagger_{\mathrm{L}\downarrow}d^\dagger_{R\uparrow}) \right. \tag{7}$$

$$\left. + (1-\phi)(d^\dagger_{\mathrm{L}\uparrow}d^\dagger_{\mathrm{L}\downarrow} + d^\dagger_{\mathrm{R}\downarrow}d^\dagger_{\mathrm{R}\uparrow})\right]|0\rangle\,, \tag{8}$$

which clearly shows that the interaction parameter ϕ determines whether the two electrons are in an entangled state (for $\phi = 1$) or not (for $\phi = 0$). Consequently, one obtains for the concurrence (3) [22]

$$\mathcal{C} = \frac{2\phi}{1+\phi^2}\,, \tag{9}$$

which varies between 0 and 1 as a function of the parameter $\phi \in [0, 1]$. This example nicely shows the correspondence between the abstract entanglement measure $\mathcal{C}$ and a physical implementation of two electrons in a double quantum dot. To access the parameter, one can study the average current using a master equation in the sequential tunneling limit or taking into account cotunneling as was done in Ref. [22]. Further aspects include entanglement in triple quantum dots [24], in a double-dot turnstile [25], or using Aharonov–Bohm interferometer coupled dots [26].

3.2 Transport properties – Current and noise

The transport properties are summarized in Fig. 2, which shows the average current (top panel) and the Fano factor (bottom panel) as a function of the bias voltage V and the gate voltage V_g. Considering the current, the most visible feature is the Coulomb blockade diamond (green in Fig. 2). As long as the bias voltage is lower than the energy difference between the energetically lowest state and the next state with one electron more or less, i.e., $eV < E_i(V_g) - E_j(V_g)$ with i and j being two states differing by one electron, electron tunneling is exponentially suppressed. In our model, we have three such blockade regimes with 0, 1, and 2 electrons in the dot for zero bias voltage. The two parts of Fig. 2 show the current and the Fano factor for the most interesting of these blockade regions, the one-electron blockade regime. We will concentrate our discussion on this region, since most interesting features can be discussed here.

3.3 Transport – Full counting statistics analysis

A more detailed view of the transport characteristic can be obtained by looking at the full counting statistics (FCS) [27]. The aim is here to find the cumulant generating function (CGF) $\mathcal{S}(\chi)$, which is related to the probability $P(N)$ of N charges passing through the system per unit time by $\exp \mathcal{S}(\chi) = \sum_N P(N)e^{iN\chi}$. The knowledge of $\mathcal{S}(\chi)$ is equivalent to the knowledge of all the cumulants of the system according to $C_k = (-i\partial/\partial_\chi)^k \mathcal{S}(\chi)\big|_{\chi=0}$, such as current (first cumulant) and noise (second cumulant), $I = eC_1$ and $S = 2e^2C_2$, respectively (where e is the electron charge). The simplest way to evaluate the counting statistics in this case is to use the method described in Ref. [27]. We choose (without loss of generality) to count the charges in the left lead. Therefore, we have to change the left tunneling rates in the off-diagonal elements of the transport matrix $\mathbf{M}$: $\Gamma_L \to \Gamma_L \exp(i\chi)$. The smallest eigenvalue of $\mathbf{M}$, which we denote by $\lambda_0(\chi)$, determines the CGF as $\mathcal{S}(\chi) = -\lambda_0(\chi)$.

If we restrict our calculations to a certain region and thus reduce the number of involved states, it is possible to get an analytical expression for the Fano factor [28]. For region C, we include the one-electron states $|+\rangle$, $|-\rangle$, and the two-electron singlet $|S\rangle$, while other (e.g., triplet) states are outside. This means in practice that the dots interact with each other, so they are not fully separated (communication loophole). Here, the relevant energy differences are both smaller than the bias: $E_S - E_- < E_S - E_+ < eV/2$. Therefore, both Fermi functions for the tunneling processes are exponentially suppressed, but one is much bigger than the other:

$$1 \gg f(E_S - E_+ - eV/2) \gg f(E_S - E_- - eV/2)\,. \tag{10}$$

Therefore, we neglect $f(E_S - E_- - eV/2)$ and take the rates to lowest order in the parameter $x \equiv f(E_S - E_+ - eV/2)$.

Then the tunneling rates are

$$\Gamma_{+S} \approx \frac{1}{1+\phi^2}\gamma_L x, \quad \Gamma_{S+} \approx \frac{2}{1+\phi^2}(\gamma_L+\gamma_R),$$
$$\Gamma_{-S} \approx \frac{\phi^2}{1+\phi^2}\gamma_L, \quad \Gamma_{S-} \approx \frac{2\phi^2}{1+\phi^2}(\gamma_L+\gamma_R).$$

Here $\gamma_{L/R}$ are the bare tunneling rates for the left/right leads. Without loss of generality, we will count the charges in the left lead, which means that we have to replace $\gamma_L \leftrightarrow \gamma_L \exp(\pm i\chi)$ (the sign depending on whether an electron enters or leaves the dot, respectively) in the off-diagonal elements of the matrix $\mathbf{M}$. The counting statistics is obtained from the smallest eigenvalue λ_0, which we determine to lowest order in x. The result is

$$\mathcal{S}(\chi) = -x\frac{\gamma_L\gamma_R(1+\phi^2)}{\gamma_R(1+\phi^2)-\gamma_L}\frac{e^{i\chi}-1}{1-p(\phi)e^{i\chi}}, \tag{11}$$

where $p(\phi) = \phi^2\gamma_R/[\gamma_L+\gamma_R(1+\phi^2)]$. Finally, we obtain the Fano factor

$$F(\phi) = \frac{1+p(\phi)}{1-p(\phi)} = 1+\phi^2\frac{2\gamma_R}{\gamma_L+\gamma_R}, \tag{12}$$

which is independent of the bias voltage as long as we are in the one-electron Coulomb blockade regime. For a symmetric structure with $\gamma_L = \gamma_R$, we obtain

$$F(\phi) = 1+\phi^2. \tag{13}$$

Note that in both cases discussed here the Fano factor is super-Poissonian, viz. larger that 1, due to an effect similar to the dynamical channel blockade [28–31]. Hence, a measurement of the noise in this regime allows a direct determination of the interaction parameter ϕ. That such measurements are possible has been demonstrated experimentally [32–34]. In future, it seems interesting to investigate further ways to assess the entanglement.

4 Entanglement at quantum point contacts

Non-interacting fermions in the Fermi sea can get entangled due to the Pauli exclusion principle. In contrast, non-interacting bosons cannot get entangled by means of linear manipulations (e.g., beam splitters) out of vacuum or thermal states [35]. In contrast, entangled electron–hole pairs, in the form of the Bell state (1), are created at both sides of a biased tunnel junction [35–48, 69]. So far the efforts concentrated on testing entanglement by second-order current correlations [36–49]. Entanglement is supposed to be present if the inequality

$$|c(A_1B_1)+c(A_1B_2)+c(A_2B_1)-c(A_2B_2)| \le 2 \tag{14}$$

is violated. Here the correlators are defined as $c(A,B) = \langle A^-B^-\rangle/\langle A^+B^+\rangle$, with $\hat{A}^\pm = \hat{P}_{A+} \pm \hat{P}_{A-}$. The projections $\hat{P}_\pm$ are on disjoint subspaces. The definition (14) has the advantage of eliminating the detection loophole. If only a small fraction is detected the observable becomes $\hat{A}^\pm \to \alpha\hat{A}^\pm$, whereas the inequality (14) is unaffected by a small α. However, it differs from the standard setup for the Bell inequality where the dichotomy of the outcomes can be verified experimentally by the check $A^2 = B^2 = 1$, which is verified in single-photon-counting detectors.

The dichotomy in (14), instead of being directly experimentally tested, is simply assumed in the quantum description of projections. Moreover, in the picture of electron–hole pairs created at the junction, the corresponding operators $\hat{A}$ and $\hat{B}$ entering quantum averages $\langle\hat{A}\hat{B}\rangle$ are time integrals over electric current, $\hat{A}^\pm = \int dt(\hat{I}_{A1}(t) \pm \hat{I}_{A2}(t))$, $\hat{A} = \hat{A}^-$, while current operators $\hat{I}_A$ and $\hat{I}_B$ usually do not commute and do not project. Consequently, an interpretation of current measurements needs to take into account the measurement scheme, e.g., in terms of weak measurements [50–52]. Unfortunately, to make the (Bell) test non-classicality convincing, the dichotomy (equivalent here to charge flow quantization) must be verified directly in the measurements. However, in tunnel junctions and quantum point contacts rather cumulants of the electric current are directly accessible and, so far, the noise [53–55] and the third cumulant [56–58] of the current have been measured. The main problem is a large background noise, which hampers the extraction of the real correlations, especially when going to higher than second moments. The quantization of charge flow is also not so evident at short time scales or high frequencies, when vacuum fluctuations of the Fermi sea play a role [59–62].

4.1 Weak positivity

The bad news for experimentalists trying to perform the Bell test at point contacts is that first- and second-order correlation functions can always be reproduced classically [63]. To see this, consider a real symmetric correlation matrix $2C_{ij} = 2\langle A_iA_j\rangle = \mathrm{Tr}\hat{\rho}\{\hat{A}_i,\hat{A}_j\}$ with $\{\hat{A},\hat{B}\} = \hat{A}\hat{B}+\hat{B}\hat{A}$ for arbitrary, even non-commuting, observables $\hat{A}_i$ and density matrix $\hat{\rho}$. This includes all possible first-order averages $\langle A_i\rangle$ by setting one observable to the identity. Since $\mathrm{Tr}\hat{\rho}\hat{X}^2 \ge 0$ for $\hat{X} = \sum_i \lambda_i\hat{A}_i$ with arbitrary real λ_i, we find that the correlation matrix C is positive definite and any (even genuine quantum) correlation can be simulated by a classical Gaussian distribution $\rho \propto \exp(-\sum_{ij} {C^{-1}}_{ij}A_iA_j/2)$. Note that the often used dichotomy $A = \pm 1$ is equivalent to $\langle(A^2-1)^2\rangle = 0$, which requires us to measure the fourth-order correlator $\langle A^4\rangle$. Moreover, every classical inequality $\langle(f(\{A_i\})^2\rangle \ge 0$ contains the highest correlator of even order. Hence, to detect non-classical effects with unbounded observables without any additional assumptions, we have to consider the fourth moments.

4.2 Fourth-moment inequality

To help experimentalists to use moments as low as possible, we should try to find a fourth-moment inequality. Such an inequality has been

proposed some time ago [64] and reads

$$\langle A_1B_1 - A_2B_2\rangle^2 + \langle A_1B_2 + A_2B_1\rangle^2 \leq \langle (A_1^2 + A_2^2)(B_1^2 + B_2^2)\rangle\,. \tag{15}$$

Unfortunately, it turns out that this inequality cannot even be violated quantum mechanically [65].

A fourth-moment inequality that holds classically but is violated in quantum mechanics is much more complicated and reads [63]

$$\begin{aligned} &2|\langle A_1B_1(A_1^2+B_1^2)\rangle + \langle A_2B_1(A_2^2+B_1^2)\rangle \\ &\quad + \langle A_1B_2(A_1^2+B_2^2)\rangle - \langle A_2B_2(A_2^2+B_2^2)\rangle| \\ &\leq 2\left(\langle A_1^4\rangle + \langle A_2^4\rangle + \langle B_1^4\rangle + \langle B_2^4\rangle\right) \\ &\quad + \sum_{X,Y,Z=\{A_{1,2},B_{1,2}\}}^{Y\neq X;Z\neq X,Y,Y'} (\langle X^4\rangle\langle Y^4\rangle)^{1/4}\langle (Y^2-Z^2)^2\rangle^{1/2}\,, \end{aligned} \tag{16}$$

where $Y_i' = Y_{3-i}$. For dichotomic outcomes $A_{1,2}^2 = B_{1,2}^2 = 1$ it reduces to the Bell inequality (5) and can be violated in a standard way.

4.3 Proposal for experiments Now we implement the Bell example in a beam-splitting device involving fermions scattered at a tunnel junction. The junction is described by fermionic operators around the Fermi level [66, 67]. Each operator $\hat\psi_{A\bar n}$ is denoted by mode number $n \in \{1, ..., N\}$ and spin orientation $\sigma = \uparrow, \downarrow$, $\bar n = (n, \sigma)$, and $A = L, R$ for left- and right-going electrons, respectively. Each mode has its own Fermi velocity v_n and transmission coefficient $\mathcal{T}_n$ (reflection $\mathcal{R}_n = 1 - \mathcal{T}_n$). We will assume non-interacting electrons and energy- and spin-independent transmission through the junction. The Hamiltonian is

$$\begin{aligned} \hat H = \sum_{\bar n}\int \mathrm{d}x\,\{ &i\hbar v_n[\hat\psi_{L\bar n}^\dagger(x)\partial_x\hat\psi_{L\bar n}(x) - L\leftrightarrow R] \\ &+ eV\theta(-x)[\hat\psi_{L\bar n}^\dagger(x)\hat\psi_{L\bar n}(x) + L\leftrightarrow R] \\ &+ q_n\delta(x)[\hat\psi_{L\bar n}^\dagger(x)\hat\psi_{R\bar n}(-x) + \hat\psi_{R\bar n}^\dagger(x)\hat\psi_{L\bar n}(-x)]\}\,. \end{aligned} \tag{17}$$

The fermionic operators satisfy anticommutation relations $\{\hat\psi_a(x), \hat\psi_b(x')\} = 0$ and $\{\hat\psi_a(x), \hat\psi_b^\dagger(x')\} = \delta_{ab}\delta(x - x')$ for $a, b = L\bar n, R\bar m$. The transmission coefficients are $\mathcal{T}_n = \cos^2(q_n/\hbar v_n)$. The system's current operator is defined as $\hat I_n(x) = \sum_\sigma ev_n\hat\psi_{L\bar n}^\dagger(x)\hat\psi_{L\bar n}(x) - L\leftrightarrow R$ and the density matrix is $\hat\rho \propto \exp(-\hat H/k_BT)$.

The effect of each part of the Hamiltonian on the single-mode wave function can be described by three scattering matrices [66, 67] (see the setup in Fig. 3)

$$s_i = \begin{pmatrix} r_i & t_i \\ t_i' & r_i' \end{pmatrix}\,, \tag{18}$$

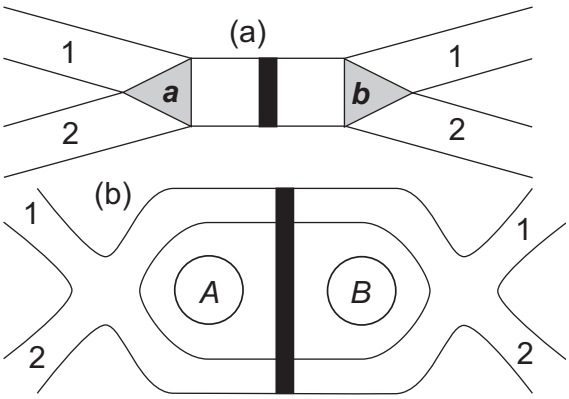

Figure 3 Proposals of experimental setup for the Bell test. In both cases the black bar represents the scattering barrier, producing entangled electron–hole pairs. The tested observable is the difference of currents, $I_1 - I_2$, at the left (Alice) or the right (Bob) side. The correlations depend on the spin scattering (a) or the magnetic fluxes (b).

where $i = A, T, B$ describe scattering at the left detector, junction, and right detector, respectively. The junction has diagonal transmission and reflection submatrices, with $t_T = t_T' = i\sqrt{\mathcal{T}}\hat 1$. If the junction is prepared at zero temperature with the voltage bias eV, then the outgoing scattering state takes the simplified form

$$\begin{aligned} &(1-\mathcal{T})|0\rangle - \mathcal{T}\,|\uparrow\downarrow\rangle_h\,|\uparrow\downarrow\rangle_e \\ &\quad - \sqrt{2\mathcal{T}(1-\mathcal{T})}(|\uparrow\rangle_h\,|\uparrow\rangle_e + |\downarrow\rangle_h\,|\downarrow\rangle_e)/\sqrt{2}\,, \end{aligned} \tag{19}$$

where $|0\rangle$ denotes the initial state (as if the barrier was closed), h denotes the "hole" state on the lower-voltage side, while e denotes the "electron" state on the higher-voltage side. The last part of the state is entangled analogously to (1). The rate (frequency) of production of entangled electron–hole pairs is given by $2eV/\mathcal{T}(1-\mathcal{T})$. The entanglement can be destroyed by temperature. The maximal (critical) temperature k_BT_c for entanglement is found from the relation [35]

$$\mathcal{T}(1-\mathcal{T})\sinh^2(eV/2k_BT) = 1/4\,, \tag{20}$$

with the highest value $k_BT_c \simeq 0.57eV$ for $\mathcal{T} = 1/2$.

The presence of entanglement can be shown by violation of Bell-type inequalities (14) (of course with the experimentally unverified assumptions about the representation of operators) or (16). The Bell measurement will be performed by adding spin filters or magnetic flux at both sides of the junctions as shown in Fig. 3. In both cases we have to add $\hat H' = \sum_{ab}\int \mathrm{d}x\, eV_{ab}(x)\hat\psi_a^\dagger(x)\hat\psi_b(x)$ to the Hamiltonian (17), where $V_{ab}(x)$ is the scattering potential, localized near the detectors.

In the case of spin filters we assume a 4×2 transmission matrix $t_A = (1 + \boldsymbol{a}\cdot\hat{\boldsymbol{\sigma}}\;\; 1 - \boldsymbol{a}\cdot\hat{\boldsymbol{\sigma}})/2$, where $|\boldsymbol{a}| = 1$. Alternatively, we could introduce 'artificial spin' filters, taking $\sigma_{1,3}$ acting in the mode space instead of spin space, hav-

ing a magnetic-flux-tunable geometry of the scatterer. For magnetic fluxes we assume $r_A = 0$ and

$$t_A = \begin{pmatrix} e^{i\phi_A} & 0 \\ 0 & 1 \end{pmatrix} \frac{1}{\sqrt{2}} \begin{pmatrix} 1 & 1 \\ 1 & -1 \end{pmatrix}, \tag{21}$$

where ϕ_A represents the Aharonov–Bohm phase picked up on the upper branch. The matrices can be enlarged to represent $2N$-mode junctions. In both cases, the transmission coefficients for the total scattering matrix are $\mathcal{T}_{11} = \mathcal{T}_{22} = \mathcal{T}(1 + \boldsymbol{a}\cdot\boldsymbol{b})/2$ and $\mathcal{T}_{12} = \mathcal{T}_{21} = \mathcal{T}(1 - \boldsymbol{a}\cdot\boldsymbol{b})/2$ where $\boldsymbol{a} = (\cos\phi_A, \sin\phi_A, 0)$ in the case of magnetic fluxes.

As in the existing proposals [35–48], the tunnel barrier produces electron–hole pairs with entangled spins or orbitals. Alice and Bob can test the inequality (16) by measuring the difference between the charge flux in the upper and the lower arms as shown in Fig. 3. For Alice, the measured observable in the Heisenberg picture reads

$$\hat{A}^{\pm} = \int \mathrm{d}t\; f(t)(\hat{I}_1(x_A, t) \pm \hat{I}_2(x_A, t))/e,\;\; \hat{A} = \hat{A}^{-} \tag{22}$$

for the filter setting $\boldsymbol{a}$. Here x_A is the point of measurement, satisfying $\max\{|eV|, k_\mathrm{B}T\}|x_A/v_n\hbar| \ll 1$ with $f(t)$ slowly changing on the time scale $\hbar/\max\{|eV|, k_\mathrm{B}T\}$. One defines analogously B for Bob.

The measured probability distribution can be treated as a convolution $\rho = \rho_\mathrm{d} \times \varrho$, where ρ_d is the Gaussian detection noise – independent of the system and later subtracted. ϱ is a quasiprobability [50–52] and averages are defined as

$$\begin{aligned} &\langle X_1(t_1)\cdots X_n(t_n)\rangle_\varrho \\ &\quad = \mathrm{Tr}\hat{\rho}\{\hat{X}_1(t_1), \{\cdots\{\hat{X}_{n-1}(t_{n-1}), \hat{X}_n(t_n)\}\cdots\}\}/2^{n-1} \end{aligned} \tag{23}$$

for time-ordered observables, $t_1 \le t_2 \le \cdots \le t_n$. The detection noise adds $I_{\mathrm{d}i}$ to the measurement outcome I_i with $\langle I_{\mathrm{d}i}(0)I_{\mathrm{d}j}(t)\rangle = e^2\delta(t)\delta_{ij}/\tau$. In the non-interacting limit (the sensitivity τ much smaller than the time resolution of the measurement – the time scale on which $f(t)$ is finite), one can calculate averages with respect to ϱ using existing methods, based on FCS and its extension [63]. We have $\langle A\rangle_\varrho = \langle B\rangle_\varrho = 0$ and $\langle AB^3\rangle_\varrho = \langle A^3B\rangle_\varrho = (\boldsymbol{a}\cdot\boldsymbol{b})\langle A^4\rangle_\varrho$ and $\langle A^4\rangle_\varrho = \langle B^4\rangle_\varrho$. The inequality (16) gets a simplified form in this particular case,

$$|C(\boldsymbol{a}_{1,2}, \boldsymbol{b}_{1,2})| \le 2 + 4\sqrt{2\left(1 - \frac{\langle A^2B^2\rangle_\varrho}{\langle A^4\rangle_\varrho}\right)}, \tag{24}$$

where $C(\boldsymbol{a}_{1,2}, \boldsymbol{b}_{1,2}) = \boldsymbol{a}_1\cdot\boldsymbol{b}_1 + \boldsymbol{a}_2\cdot\boldsymbol{b}_1 + \boldsymbol{a}_1\cdot\boldsymbol{b}_2 - \boldsymbol{a}_2\cdot\boldsymbol{b}_2$. We stress that (24) follows from theoretical predictions and the experimental test still requires the measurement of all averages in (16). We choose $f(t) = \theta_\delta(2t_0 - |t|)$, where $\theta_\delta(t) = \theta(t)$ for $|t| \gg \delta$ with a smooth crossover at $|t| \lesssim \delta$.

Having assumed the tunneling limit ($\mathcal{T} \ll 1$), we make the following approximations:

$$1/N\mathcal{T} \gg t_0\max\{|eV|, k_\mathrm{B}T\}/h \gg t_0/\delta \gg 1\,, \tag{25}$$

with $2N$ denoting the total number of modes going through the barrier. In this limit, one obtains a simple physical picture: the electron–hole Bell pairs are transmitted according to Poissonian statistics, with all moments equal:

$$\langle A^{2n}B^{2m}\rangle_\varrho \simeq \frac{2eVN\mathcal{T}t_0}{h}\coth\left(\frac{eV}{2k_\mathrm{B}T}\right),\; n+m>0 \tag{26}$$

and also $\langle A^+B^+\rangle_\varrho \simeq \langle A^{2n}B^{2m}\rangle_\varrho$ Hence, the last term on the right-hand side of Eq. (24) is negligible and the inequalities (14) and (16) take the usual form $|C(\boldsymbol{a}_{1,2}, \boldsymbol{b}_{1,2})| \le 2$, which can be violated by appropriate choice of the spin axes. Instead of measuring in the time domain, one can measure correlations in the frequency domain (up to $\omega \sim 1/t_0$) and make the Fourier transform. If the scattering is mode-independent then one can assume that the junction consists of minimally $N_0 \simeq Gh/e^2$ independent channels, where $G = 2N\mathcal{T}e^2/h$ is the total conductance of the junction, and repeat the whole above reasoning with N replaced by N/N_0 (experimentally – dividing measured cumulants $\langle\langle\cdots\rangle\rangle$ by N_0).

We should stress, however, that the violation of (14) or (16) is here possible also at finite temperature but zero voltage, where no entanglement is predicted by (20) [68]. This is because the measurements are performed very close to the junction, where Alice and Bob are too close to claim any non-locality or separability, and the detection noise is subtracted (equivalent to the detection loophole). For the measurements far enough away from the junctions, there are additional contributions to the moments, not proportional to $\mathcal{T}$ and leading to intrinsic additional detection noise, which destroy the violation of Ref. [63]. This is why one should continue to search for better tests of entanglement and nonlocality at point contacts and tunnel junctions, reducing also the detection noise.

5 Hierarchy of mesoscopic Bell test In the previous section we have discussed several aspects of entanglement verification using current measurements in semiconductor nanostructures. We now compare several ways to extract the entanglement produced in a given setup. It is important to keep in mind that many experimental setups require additional assumptions. Depending on how severe these assumptions are, we propose a hierarchy of entanglement tests. The several steps to achieve trust in a given entanglement test are summarized in Table 1.

The first and simplest test is to map the entanglement properties on quantities, which determine the average current. This was, for example, done in Refs. [22, 23], where the important interaction parameter ϕ at the same time determines the entanglement in the form of the concurrence and

Table 1 Hierarchy of entanglement tests.

mesoscopic Bell tests	entanglement security
testing non-local influence on conductance (easily done, but strong theoretical input and not conclusive test of entanglement)	
crossed Andreev signal in a non-local conductance measurement (test of single-particle property only, needs theory input)	
testing the angular spin dependence of cross correlations (trust in the full counting statistics)	
Bell test with second-order correlations directly (however very fast and at very low temperatures)	
assumption-free Bell test with fourth-order correlations (works for any system, all "loopholes" are excluded)	

several transport properties, like current and noise. For example, a study of the complete gate and bias voltage dependence allows us to confirm the electronic spectrum of the quantum dot in great detail. Hence, one can believe in the presence of entangled two-electron states. However, the biggest drawback is that everything is rather local, since the two orbital states in the quantum dot even have overlapping wave functions. Whether or not the entangled electrons can be spatially separated cannot be decided on the basis of such measurements.

A generic entangler consists of a source and two leads into which the two partners of an EPR pair propagate. In terms of electronic circuits, this means that we speak about a three-terminal device, which is described by a conductance matrix, setting the proportionality between currents and bias voltages and defined by $I_i = \sum_j G_{ij} V_j$. We assume here for simplicity that we stay in the linear response regime. A first test of locality [20, 21] is to check that the local conductances G_{ii} depend on changing a parameter at another terminal, e.g., by applying local gate voltages. As before the interpretation of such local conductance measurement relies heavily on modeling. However, information on the efficiency of the splitting of an entangled pair has been obtained in that manner. It is important to check the details of the model with some control measurements, like, e.g., interchanging control and measurement terminals, which have not been performed. Nevertheless, there is hope to achieve a highly efficient splitting [70]. The next level would be to measure the non-local conductance, e.g., by injecting a current through one contact and measuring the voltage at the other normal lead. Such a setup has been investigated in the context of crossed Andreev reflection [71–73], which is the microscopic mechanism responsible for non-local processes and contributing to the non-local conductances G_{ij} for $i \neq j$. However, experimental tests have been hampered by a large contribution of direct electron transfer [73–76]. Most recently it was proposed that entanglement can be detected in conductance measurements alone [77, 78], which however do not allow us to exclude that, e.g., due to dephasing the entanglement has been destroyed. Furthermore, such tests assume a given setup and if those additional assumptions are not fulfilled experimentally, the corresponding inequality can be violated in the absence of entanglement.

The most obvious test of the non-local correlation is a direct measurement of two observables in distant terminals, much in the spirit of the original Bell test. In quantum transport setups, this means accessing the cross correlations of the currents at different terminals. One central problem with such tests is that the current measured is usually averaged over some time interval which is much longer than the mean time between single events. The same is of course true for correlation measurements. Hence, the observables are the time-averaged current operators, which cannot be simply mapped to spin observables as is required for the Bell test in the Clauser-Horne-Shimoni-Holt (CHSH) [5, 6] formulation. This can be simply seen from the definitions around (14), for which the operator identity $\hat{A}^2 = 1$ is not fulfilled, even after normalization. A first test could access the dependence of the cross-correlation signal on the mutual angle between the spin polarizations of the detectors. Note that the spin can equally well replaced by any other effective dichotomic degree of freedom, like different channels, valleys, or similar. The quantum prediction of the cross correlation $C(\boldsymbol{a}, \boldsymbol{b}) \sim -\boldsymbol{a} \cdot \boldsymbol{b}$ can be checked for all angles and thus constitutes not only a check of the detection efficiency, but also hints to the fact that the current is essentially bound to a total spin $S = 0$. However, such a result could still be produced by classically correlated particles, simply because the detection scheme is too slow to extract only the coincidences. A next step is to try to violate some sort of Bell inequality by mapping the observables onto some pseudo-spin observable, which reduces to the spin algebra for dichotomic outcomes. The main problem here is that the mapping only works in limiting cases, for example, at zero temperature, where the currents are bound to maximal values determined by ballistic transmission. However, since such values depend on the measuring time, in general they have to be normalized by some other measurable quantity like the average current. These observables lead to unbound fluctuations at finite temperature, which might lead to a fake violation of the Bell

inequality even at high temperatures [68]. This effect is a manifestation of the weak positivity and therefore does not represent a conclusive Bell test. We note that in addition the stringent conditions on the measurement time which have to be met to violate the Bell inequality even using favorable conditions and negligible temperature. The measurement time has to be so short so that it amounts to single-particle detection, which can be reached in principle by rare emission events of entangled pairs. This however at the same time reduces the performance of a possible entangler, since the emission becomes essentially fully random.

Finally, the fully conclusive Bell test requires us to go beyond second-order correlations [52], the reason being the weak positivity. It is possible to derive an inequality involving a fourth-order correlation function [52], which reduces to the Bell inequality for dichotomic observables. Furthermore, one can apply it to a tunnel junction entangler similar to the ones studied above. It turns out that the Bell-type inequality (16) is usually drastically harder to violate when the right-hand side depends on the system setup and external parameters like the temperature. Only in the case of a tunnel junction at very low temperatures can one achieve a violation, since the right-hand side of the Bell-type inequality (16) approaches the dichotomic limit. To summarize, we note that making entanglement a useful resource for quantum computation requires such a detailed control of the quantum correlations, so that the high-frequency and ultra-short temporal control of quantum correlations necessary to find a violation of a fourth-order inequality should be achievable as well.

6 Conclusions In this topical review, we have discussed several aspects of entanglement in semiconductor nanostructures. After a short review of essential aspects of entanglement in a quantum information theoretical framework, we turned to entanglement generation in semiconductors and related setups. We discussed the correlations in a double quantum dot, which can be related to certain entanglement measures. An entanglement detection via current and noise measurement should be feasible, as shown by a FCS analysis. Next we turned to the more general equations of correlations in general entangler setups, realized in semiconductor and/or superconducting entanglers. We have discussed that a completely new view of entanglement measures is necessary, since in general the lack of single-particle observations makes the original CHSH inequality (valid for pure spins) inapplicable. The assessment of entanglement through higher-order correlation functions is in fact a necessary ingredient of all entanglement tests of a continuous variable. Whether or not such a test can be achieved in semiconductor nanostructures is presently open, but a combined experimental and theoretical effort can hopefully make it possible.

Acknowledgements The collaboration and discussions with C. Bruder and F. Bodoky are gratefully acknowledged. Furthermore, we acknowledge discussions with Wolf-Rüdiger Hannes, Mikhail Titov, Carlo Beenakker, Markus Büttiker, Peter Samuelsson, and Yuli V. Nazarov. This work was financially supported by the German Science Foundation (DFG) through the Priority Program 1285 Semiconductor Spintronics and the SFB 767 Controlled Nanosystems.

References

[1] G. A. Prinz, Science **282**, 1660 (1998).
[2] D. D. Awshalom, D. Loss, and N. Samarth (eds.), Semiconductor Spintronics and Quantum Computation (Springer, Berlin, 2002).
[3] A. Cottet, T. Kontos, S. Sahoo, H. T. Man, M.-S. Choi, W. Belzig, C. Bruder, A. F. Morpurgo, and C. Schönenberger, Semicond. Sci. Technol. **21**, S78 (2006).
[4] A. Einstein, B. Podolsky, and N. Rosen, Phys. Rev. **47**, 777 (1935).
[5] J. S. Bell, Physics **1**, 195 (1964).
[6] J. F. Clauser, M. A. Horne, A. Shimony, and R. A. Holt, Phys. Rev. Lett. **23**, 880 (1969).
[7] A. Aspect, J. Dalibard, and G. Roger, Phys. Rev. Lett. **49**, 1804 (1982).
[8] W. Tittel, J. Brendel, H. Zbinden, and N. Gisin, Phys. Rev. Lett. **81**, 3563 (1998).
[9] M. Giustina, A. Mech, S. Ramelow, B. Wittmann, J. Kofler, J. Beyer, A. Lita, B. Calkins, T. Gerrits, S. W. Nam, R. Ursin, and A. Zeilinger, Nature (London) **497**, 227 (2013).
[10] M. A. Nielsen and I. L. Chuang, Quantum Computation and Quantum Information (Cambridge University Press, Cambridge, 2000).
[11] D. Loss and D. DiVincenzo, Phys. Rev. A **57**, 120 (1998).
[12] G. Burkard, D. Loss, and D. P. DiVincenzo, Phys. Rev. B **59**, 2070 (1999).
[13] P. Recher, E. V. Sukhorukov, and D. Loss, Phys. Rev. B **63**, 165314 (2001).
[14] R. Werner, Phys. Rev. A **40**, 4277 (1989).
[15] W. K. Wootters, Quantum Inf. Comput. **1**, 27 (2001).
[16] W. K. Wootters, Phys. Rev. Lett. **80**, 2245 (1998).
[17] G. Weihs, T. Jennewein, C. Simon, H. Weinfurter, and A. Zeilinger, Phys. Rev. Lett. **81**, 5039 (1998).
[18] D. N. Matsukevich, P. Maunz, D. L. Moehring, S. Olmschenk, and C. Monroe, Phys. Rev. Lett. **100**, 150404 (2008).
[19] H. O. H. Churchill, A. J. Bestwick, J. W. Harlow, F. Kuemmeth, D. Marcos, C. H. Stwertka, S. K. Watson, and C. M. Marcus, Nature Phys. **5**, 321 (2009).
[20] L. Hofstetter, S. Csonka, J. Nygård, and C. Schönenberger, Nature (London) **461**, 960 (2009).
[21] L. G. Herrmann, F. Portier, P. Roche, A. Levy Yeyati, T. Kontos, and C. Strunk, Phys. Rev. Lett. **104**, 026801 (2010).
[22] V. N. Golovach and D. Loss, Phys. Rev. B **69**, 245327 (2004).
[23] F. Bodoky, W. Belzig, and C. Bruder, Phys. Rev. B **77**, 035302 (2008).
[24] D. S. Saraga and D. Loss, Phys. Rev. Lett. **90**, 166803 (2003).
[25] X. Hu and S. Das Sarma, Phys. Rev. B **69**, 115312 (2004).
[26] S. Legel, J. König, and G. Schön, New J. Phys. **10**, 045016 (2008).
[27] D. A. Bagrets and Yu. V. Nazarov, Phys. Rev. B **67**, 085316 (2003).
[28] W. Belzig, Phys. Rev. B **71**, 161301(R) (2005).
[29] A. Cottet and W. Belzig, Europhys. Lett. **66**, 405 (2004).
[30] A. Cottet, W. Belzig, and C. Bruder, Phys. Rev. Lett. **92**, 206801 (2004).

[31] A. Cottet, W. Belzig, and C. Bruder, Phys. Rev. B **70**, 115315 (2004).
[32] L. DiCarlo, H. J. Lynch, A. C. Johnson, L. I. Childress, K. Crockett, C. M. Marcus, M. P. Hanson, and A. C. Gossard, Phys. Rev. Lett. **92**, 226801 (2004).
[33] Y. Zhang, L. DiCarlo, D. T. McClure, M. Yamamoto, S. Tarucha, C. M. Marcus, M. P. Hanson, and A. C. Gossard, Phys. Rev. Lett. **99**, 036603 (2007).
[34] D. T. McClure, L. DiCarlo, Y. Zhang, H.-A. Engel, C. M. Marcus, M. P. Hanson, and A. C. Gossard, Phys. Rev. Lett. **98**, 056801 (2007).
[35] C. W. J. Beenakker, Proc. Int. School Phys. E. Fermi, Vol. 162 (IOS Press, Amsterdam, 2006).
[36] D. Loss and E. V. Sukhorukov, Phys. Rev. Lett. **84**, 1035 (2000).
[37] G. Burkard, E. V. Sukhorukov, and D. Loss, Phys. Rev. B **61**, R16303 (2000).
[38] S. Kawabata, J. Phys. Soc. Jpn. **70**, 1210 (2001).
[39] G. B. Lesovik, T. Martin, and G. Blatter, Eur. Phys. J. B **24**, 287 (2001).
[40] N. M. Chtchelkatchev, G. Blatter, G. Lesovik, and T. Martin, Phys. Rev. B **66**, 161320(R) (2002).
[41] C. W. J. Beenakker, C. Emary, M. Kindermann, and J. L. van Velsen, Phys. Rev. Lett. **91**, 147901 (2003).
[42] C. W. J. Beenakker and M. Kindermann, Phys. Rev. Lett. **92**, 056801 (2004).
[43] P. Samuelsson, E. V. Sukhorukov, and M. Büttiker, Phys. Rev. Lett. **92**, 026805 (2004).
[44] A. V. Lebedev, G. B. Lesovik, and G. Blatter, Phys. Rev. B **71**, 045306 (2005).
[45] A. Di Lorenzo and Y. V. Nazarov, Phys. Rev. Lett. **94**, 210601 (2005).
[46] H. Wei and Y. V. Nazarov, Phys. Rev. B **78**, 045308 (2008).
[47] P. Samuelsson, I. Neder, and M. Büttiker, Phys. Rev. Lett. **102**, 106804 (2009).
[48] C. Emary, Phys. Rev. B **80**, 161309(R) (2009).
[49] J. Wei and V. Chandrasekhar, Nature Phys. **6**, 494 (2010).
[50] A. Bednorz and W. Belzig, Phys. Rev. Lett. **101**, 206803 (2008).
[51] A. Bednorz and W. Belzig, Phys. Rev. Lett. **105**, 106803 (2010).
[52] A. Bednorz and W. Belzig, Phys. Rev. B **81**, 125112 (2010).
[53] M. I. Reznikov, M. Heiblum, H. Shtrikman, and D. Mahalu, Phys. Rev. Lett. **75**, 3340 (1995).
[54] A. Kumar, L. Saminadayar, D. C. Glattli, Y. Jin, and B. Etienne, Phys. Rev. Lett. **76**, 2778 (1996).
[55] R. J. Schoelkopf, P. J. Burke, A. A. Kozhevnikov, D. E. Prober, and M. J. Rooks, Phys. Rev. Lett. **78**, 3370 (1997).
[56] B. Reulet, J. Senzier, and D. Prober, Phys. Rev. Lett. **91**, 196601 (2003).
[57] Y. Bomze, G. Gershon, D. Shovkun, L. S. Levitov, and M. Reznikov, Phys. Rev. Lett. **95**, 176601 (2005).
[58] G. Gershon, Y. Bomze, E. V. Sukhorukov, and M. Reznikov, Phys. Rev. Lett. **101**, 016803 (2008).
[59] E. Zakka-Bajjani, J. Ségala, F. Portier, P. Roche, and D. C. Glattli, Phys. Rev. Lett. **99**, 236803 (2007).
[60] E. Zakka-Bajjani, J. Dufouleur, N. Coulombel, P. Roche, D. C. Glattli, and F. Portier, Phys. Rev. Lett. **104**, 206802 (2010).
[61] J. Gabelli and B. Reulet, Phys. Rev. Lett. **100**, 026601 (2008).
[62] J. Gabelli and B. Reulet, J. Stat. Mech. P01049 (2009).
[63] A. Bednorz and W. Belzig, Phys. Rev. B **83**, 125304 (2011).
[64] E. G. Cavalcanti, C. J. Foster, M. D. Reid, and P. D. Drummond, Phys. Rev. Lett. **99**, 210405 (2007).
[65] A. Salles, D. Cavalcanti, A. Acin, D. Pérez-Garcia, and M. M. Wolf, Quantum Inf. Comput. **10**(7–8), 703 (2010).
[66] Ya. M. Blanter and M. Büttiker, Phys. Rep. **336**, 1 (2000).
[67] Y. V. Nazarov and Y. M. Blanter, Quantum Transport (Cambridge University Press, Cambridge 2009).
[68] W.-R. Hannes and M. Titov, Phys. Rev. B **77**, 115323 (2008).
[69] I. Neder, N. Ofek, Y. Chung, M. Heiblum, D. Mahalu, and V. Umansky, Nature **448**, 333 (2007).
[70] J. Schindele, A. Baumgartner, and C. Schönenberger, Phys. Rev. Lett. **109**, 157002 (2012).
[71] G. Falci, D. Feinberg, and F. W. J. Hekking, Europhys. Lett. **54**, 255 (2001).
[72] J. P. Morten, A. Brataas, and W. Belzig, Phys. Rev. B **74**, 214510 (2006).
[73] D. Beckmann, H. B. Weber, and H. v. Löhneysen, Phys. Rev. Lett. **93**, 197003 (2004).
[74] S. Russo, M. Kroug, T. M. Klapwijk, and A. F. Morpurgo, Phys. Rev. Lett. **95**, 027002 (2005).
[75] P. Cadden-Zimansky and V. Chandrasekhar, Phys. Rev. Lett. **97**, 237003 (2006).
[76] A. Kleine, A. Baumgartner, J. Trbovic, and C. Schönenberger, Europhys. Lett. **87**, 27011 (2009).
[77] B. Braunecker, P. Burset, and A. Levy Yeyati, Phys. Rev. Lett. **111**, 136806 (2013).
[78] W. Kłobus, A. Grudka, A. Baumgartner, D. Tomaszewski, C. Schönenberger, and J. Martinek, arXiv:1310.5640 (2013).

